INTERFACE

rsif.royalsocietypublishing.org

Research

Cite this article: Gollo LL. 2017 Coexistence of critical sensitivity and subcritical specificity can yield optimal population coding. *J. R. Soc. Interface* **14**: 20170207.
http://dx.doi.org/10.1098/rsif.2017.0207

Received: 18 March 2017
Accepted: 17 August 2017

Subject Category:
Life Sciences–Physics interface

Subject Areas:
computational biology, biocomplexity, biophysics

Keywords:
diversity, heterogeneity, criticality, subcriticality, complex systems, systems neuroscience

Author for correspondence:
Leonardo L. Gollo
e-mail: leonardo.l.gollo@gmail.com

THE ROYAL SOCIETY
PUBLISHING

Coexistence of critical sensitivity and subcritical specificity can yield optimal population coding

Leonardo L. Gollo[1,2]

[1]Systems Neuroscience Group, QIMR Berghofer Medical Research Institute, Brisbane, Australia
[2]The University of Queensland, Centre for Clinical Research, Brisbane, Australia

LLG, 0000-0003-3505-9259

The vicinity of phase transitions selectively amplifies weak stimuli, yielding optimal sensitivity to distinguish external input. Along with this enhanced sensitivity, enhanced levels of fluctuations at criticality reduce the specificity of the response. Given that the specificity of the response is largely compromised when the sensitivity is maximal, the overall benefit of criticality for signal processing remains questionable. Here, it is shown that this impasse can be solved by heterogeneous systems incorporating *functional diversity*, in which critical and subcritical components coexist. The subnetwork of critical elements has optimal sensitivity, and the subnetwork of subcritical elements has enhanced specificity. Combining segregated features extracted from the different subgroups, the resulting collective response can maximize the trade-off between sensitivity and specificity measured by the dynamic-range-to-noise ratio. Although numerous benefits can be observed when the entire system is critical, our results highlight that optimal performance is obtained when only a small subset of the system is at criticality.

1. Introduction

Reliable estimations of stochastic inputs is a major challenge to many physical [1] and biological systems [2,3]. The estimation of input intensity, for instance, is fundamental for life because it constitutes the basis of sensory detection in unicellular organisms [4], single neurons [5] and animals [6]. A main issue of building a perceptual representation of inputs that arrive in a stochastic fashion derives from their unpredictable nature. Hence, the steady state of a discrete random (point) process can be easily confounded with a time-dependent one. This is also known as the gambler's fallacy [7], in which the agent (gambler) perceives a steady process as being time-varying (with hot and cold moments of luck referring to periods of short and long inter-event intervals [8]). In this case, the perception of a steady mean rate is replaced by erratic fluctuations of the signal around the mean rate. As an example, recent evidence suggests that overestimation of the volatility of the sensory environment occurs in autism [9]. Of course, the larger the amplitude of the fluctuations, the greater is the challenge to overcome this limitation to efficiently estimate the steady rate.

Critical states mediate phase transitions and exhibit numerous special features that distinguish them from other non-critical states: They have peaked correlation length [10], specific heat [11], entropy [12,13], information flow [14–17], computation [18], and so on (for a recent review, see [19] and references therein). An important practical benefit of criticality is that it exhibits maximal dynamic range [20], which means that critical systems have optimal abilities to distinguish stimulus intensity that spans several orders of magnitude. Hence, systems poised at criticality offer maximal sensitivity to detect changes in the stimulus rate [20–22]. This is particularly important to psychophysics in which variations of input must be detected for a wide range of stimulus intensities [6,20]. On the other hand, critical systems also exhibit maximal fluctuations [23,24]. This feature strongly compromises the system's specificity (the confidence of the estimated

stimulus intensity). Therefore, it is not clear whether the overall advantage of the enhanced sensitivity can overcome the limitations of reduced specificity.

To take advantage of optimal sensitivity, evidences suggest that visual [25,26] and auditory systems [27–29] operate at (or very near) critical states. However, it remains puzzling what are the workaround strategies used by living systems to overcome the blatant problem of reduced specificity that is associated with critical states. Here, we investigate sensitivity and specificity at the critical state in homogeneous and heterogeneous systems. We show that heterogeneity in node excitability leads to functional diversity, in which a subgroup of units at criticality coexists with other subgroups of subcritical units. This separation can simultaneously confer to networks the benefits of maximal sensitivity of critical units and enhanced specificity of subcritical units.

2. Methods

For concreteness we employ a general model of excitable networks [20,30,31], adapted to incorporate nodal heterogeneity [32]. Susceptible (quiescent) nodes can be excited either by (global) external driving or by (local) neighbour contributions. External inputs arrive at a steady Poisson rate h. An input rate h indicates that at each time step δt (=1 ms) an external input causing a spike may arrive with a probability $p_h = 1 - \exp(-h\delta t)$. Neighbour contributions may propagate from active units with a probability p. Active nodes become refractory in the next time step, and refractory nodes become quiescent with probability $q = 0.5$. The system is synchronously updated and the time step is fixed at 1 ms. Networks have 5000 nodes, and they are connected as a sparse Erdős–Rényi random network with average degree $K = 50$. Furthermore, diversity is introduced in the excitability threshold θ: nodes fire from neighbouring contributions if they receive at least θ inputs within one time step.

2.1. Homogeneous networks

We consider homogeneous networks in which all nodes have the same excitability threshold $\theta = 1$. This is a simple yet very influential case that highlights the benefit of criticality to enhance network sensitivity [20]. Other homogeneous networks with $\theta > 1$ may also enhance network sensitivity [32], but they come along a discontinuous phase transition and hysteresis, increasing the complexity of the dynamics. Hence, here we focus on the most standard choice of $\theta = 1$ that gives rise to a continuous phase transition [20].

2.2. Heterogeneous networks

Node diversity is a hallmark of the brain [33] that is associated with several benefits to the system [34–36]. For simplicity, diversity is introduced as a discrete uniform distribution of the threshold $\theta = 1, 2, \ldots, \theta_{\max}$. The subpopulation of most excitable units has $\theta = 1$ as in the previous case of homogeneous populations, and the least excitable subpopulation has $\theta_{\max} = 6$. Integrator units (with $\theta > 1$) become active at a lower rate than units with threshold $\theta = 1$ because they must integrate several inputs to fire.

2.3. Response function

The mean firing response F across nodes and trials is a smooth sigmoidal function of the input h that vary over orders of magnitude (figure 1*a*). This is called a response (or transfer) function. It indicates the mean output firing rate of the system for varying input rates (regularly spaced in logarithmic scale). Response functions represent a fundamental feature of the system under the rate-code framework [37].

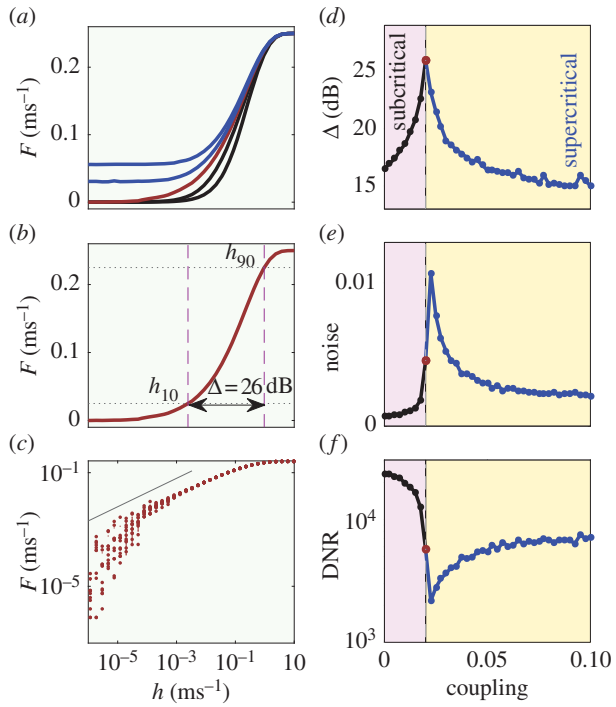

Figure 1. Maximal sensitivity and reduced specificity occurs at criticality in homogeneous networks ($\theta = 1$). (*a*) Family of response functions F for variable input h. From right to left: subcritical curves are in black ($p = 0.005$, 0.015), the critical curve is in red ($p_c = 0.02$) and supercritical curves are in blue ($p = 0.0225$, 0.025). Response functions represent an average over 10 trials. (*b*) Illustration of the dynamic range definition for the critical curve. Dashed lines indicate h_{10} and h_{90}, and dotted lines indicate F_{10} and F_{90}. (*c*) Response function variability for 10 independent trials at criticality. Grey line indicates the critical exponent $m = 0.5$. (*d*) Dynamic range as a function of the coupling strength p. (*e*) Noise, defined as the area between the confidence interval (standard deviation) over the entire response function, versus p. (*f*) Dynamic-range-to-noise ratio (Δ/noise) versus p. (Online version in colour.)

2.4. Dynamic range

A key property of response functions (shown in figure 1*a*) is the dynamic range [38]. It measures the range of stimulus intensities resulting in distinguishable network responses. The dynamic range quantifies the interval of stimulus in which the network is sensitive to small variations of input, and neglects regions of saturated responses which are too close to the minimal or maximal firing rates (saturation). Hence, dynamic range is a measure of network sensitivity that focuses on the range of stimuli in which changes are effectively detected, and influence the firing rate. Dynamic range is typically defined as $\Delta = 10\log_{10}(h_{90}/h_{10})$. In this definition [20], $h_x \equiv F^{-1}(F_x)$ corresponds to the input level of $F_x = F_0 + (x/100)(F_{\max} - F_0)$, where $F_{\max}(= 250\,\text{Hz})$ is the maximal firing rate of the network, and F_0 is the minimal firing rate of the network, or the firing rate in the absence of input $F(h = 0)$. The main elements required to compute the dynamic range of a response function are illustrated in figure 1*b*.

2.5. Noise

Another central feature of response functions is the inter-trial variability, which reflects the specificity of the network response (figure 1*c*). We quantify this *noise* by measuring the area between plus and minus one standard deviation of the mean of the response–function curves. In order to incorporate the contribution of the noise from the entire range of inputs h, this axis is first log transformed. That is, for each value of intensity the standard deviation of the firing rate across trials corresponds to the y-axis

distance in linear scale, whereas the x-axis distance is computed in logarithmic scale between regularly spaced points. Note that a linear scale in the x-axis would largely overlook the trial-to-trial variability that occurs for low values of external driving. The numerical integration was computed over the entire range of the response function using the trapezoidal rule. This is a simple and intuitive measure directly derived from response functions.

2.6. Dynamic-range-to-noise ratio

As an informative measure of the balance between sensitivity and specificity of the network response, we focus on a simple ratio: the dynamic-range-to-noise ratio (DNR). This ratio is relevant because dynamic range and noise are both basic properties of response functions. Large values of the DNR indicate a combination of sensitivity (dynamic range) and specificity of network response. The DNR is applicable and convenient when the dynamic range and the noise are greater than zero. Despite the similarity of the DNR with the traditional *signal-to-noise* ratio (SNR), there are some important differences that need to be emphasized. The noise in our definition of the DNR refers to the inter-trial variability of the response (and not to the error associated with the measure of the dynamic range). In addition, in contrast with the SNR, the DNR is designed to quantify the trade-off between sensitivity and specificity in response to the range of stimulus intensities covered by the response function. Moreover, as uncoupled units (e.g. single neurons [5]) may have non-negligible dynamic ranges, the DNR for uncoupled networks may attain large values.

2.7. Branching ratio

A typical measure of the spreading process in a network is the branching ratio σ. It is defined as $\sigma \equiv \rho(t+1)/\rho(t)$, where ρ is the fraction of active nodes, and is computed as the geometric mean over many initial conditions for each value of ρ. A branching ratio $\sigma > 1$ indicates increasing levels of activity; $\sigma < 1$ indicates decreasing levels of activity and $\sigma = 1$ indicates stable levels of activity [20].

2.8. Subnetwork perspective

In a heterogeneous network, the branching ratio, the firing rate and the response function, and its associated features (dynamic range, noise and the DNR) can be computed for each subnetwork defined by nodes that have the same threshold. It is often convenient to analyse the network in this detailed fashion because it clearly highlights the different dynamic behaviour (functional diversity) of the subpopulations.

3. Results

3.1. Sensitivity and specificity in homogeneous networks

In a homogeneous network, nodes require only one neighbouring input to activate. This homogeneous case has been subjected to numerous studies as the seminal work of Kinouchi & Copelli [20]. Response functions vary depending on the coupling strength (figure 1*a*), and strong coupling allows for self-sustained activity ($F_0 > 0$). Because response functions saturate at a similar level (h_{90}, figure 1*a*), the dynamic range (illustrated in figure 1*b*) is mostly driven by the sensitivity of the system to weak stimuli. By varying the coupling strength between nodes p, the maximum dynamic range is found at criticality ($p_c = 1/K = 0.02$). This peak shown in figure 1*d* demonstrates the optimal sensitivity of the critical state (red dot) [20].

In addition, from high sensitivity, the critical state also exhibits a large trial-to-trial variability associated with enhanced critical fluctuations. The noise curve (computed over the entire response function; see Methods) follows a trend similar to the dynamic range, with a peak close to the critical state and a fast decay away from it (homogeneous). The DNR exhibits larger values in the subcritical region, decreases near the critical state and slowly increases again in the supercritical regime as the coupling is moved away from the trough (figure 1*f*). The larger DNR at subcriticality indicates an advantage of this regime with respect to the critical and supercritical ones. This finding is compatible and also adds to other recent findings and proposals that take advantage of the subcritical regime [39–41]. Moreover, the minimal DNR occurs very close to the critical state, raising concerns about the ability of critical systems to overcome their limited specificity when the sensitivity is optimal. Is this an intrinsic and unavoidable limitation, or can it be harnessed by natural or designed systems?

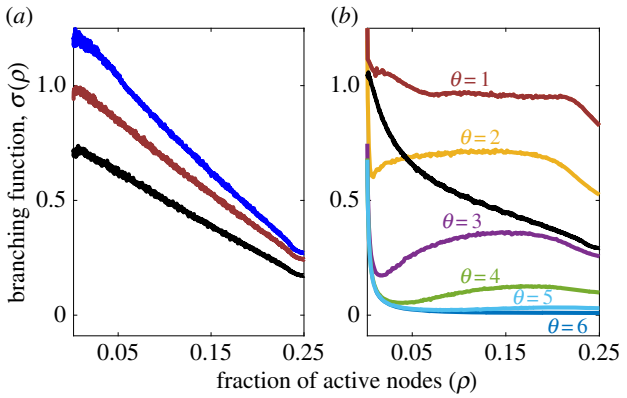

Figure 2. Branching function $\sigma(\rho)$ in homogeneous and heterogeneous systems. (*a*) Branching function decays with the fraction of active nodes (ρ). Curves represent $p = 0.025$ (blue, supercritical case), $p_c = 0.02$ (red, critical), $p = 0.015$ (black, subcritical). (*b*) Branching function in heterogeneous networks with discrete uniform distribution ($\theta = 1, 2, \ldots, 6$) at $p_c^1 = 0.14$. The branching function of the whole network is in black, and in coloured curves for subnetworks. Results obtained for different initial conditions in the absence of external driving ($h = 0$). (Online version in colour.)

3.2. Branching ratio for different dynamical regimes

To address this question, we first want to highlight the separation of the three non-overlapping regimes occurring in homogeneous systems for different coupling strengths: subcritical ($p < p_c$), critical ($p \approx p_c$) and supercritical ($p > p_c$). Each regime has a specific signature of the spreading of activity in the system [42]. As the number of quiescent nodes decays owing to larger numbers of active and refractory nodes, the branching ratio also decays with ρ (figure 2*a*).

In the subcritical state, $\sigma(\rho)$ is consistently less than one, thereby the network activity quickly vanishes in the absence of external input (figure 2*a*). At criticality, $\sigma \approx 1$ for small ρ, allowing large critical fluctuations that eventually drives the network activity to cease [43]. Network activity grows ($\sigma > 1$) in the supercritical regime for small ρ and stabilizes ($\sigma \approx 1$) at a level of self-sustained activity consistent with F_0. In all cases, nodes behave similarly because they are governed by the same rules. Additionally, as the subcritical regime shows a clear enhancement of the DNR (figure 1*f*), one possibility to overcome the limitation of the DNR at criticality comes from diversity where some nodes are at criticality and the remainder are subcritical.

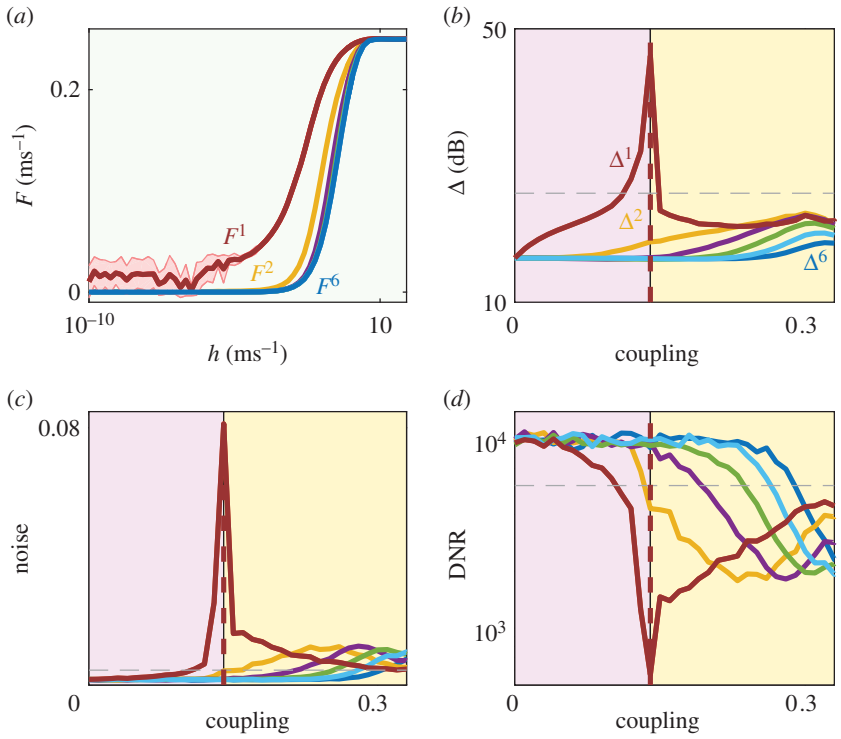

Figure 3. Maximal sensitivity and minimal specificity occurs at criticality in heterogeneous networks ($\theta_{max} = 6$). (*a*) Family of response functions F for the different subpopulations F^{θ} as a function of h for $p_c^1 = 0.14$. Subpopulations are ordered from left to right. (*b*) Dynamic range as a function of the coupling strength for the subpopulations Δ^{θ}. (*c*) Noise as a function of the coupling strength. (*d*) Dynamic-range-to-noise ratio as a function of the coupling strength. Horizontal dashed lines indicate the corresponding values at criticality for the homogeneous system of figure 1. Red dashed lines indicate the critical coupling for the subpopulation of $\theta = 1$, p_c^1. (Online version in colour.)

3.3. Response of heterogeneous networks

Integration ($\theta > 1$) makes the transmission of activity less reliable [44], which reduces the branching ratio of these subpopulations (figure 2*b*). Compared with the homogeneous case, networks in the presence of diversity require stronger coupling to reach a critical state, which vary for the different subpopulations (multiple-percolation [36,45]). For the critical state (p_c^1) of the subpopulation with $\theta = 1$, the branching ratio of this most excitable subpopulation is $\sigma \approx 1$ for a large range of ρ, and less than one for the other subpopulations. While the branching ratio for the whole network (black curve of figure 2*b*) resembles the monotonic decay of homogeneous networks (figure 2*a*), the subpopulations exhibit distinct behaviour for the same coupling strength, which leads to functional diversity.

The response functions of the subpopulations in heterogeneous systems are also very different (figure 3*a*). At p_c^1, whereas the subpopulations of integrators ($\theta > 1$) are in the subcritical state, the subpopulation with $\theta = 1$ is in the critical state. For this critical subpopulation both the dynamic range (figure 3*b*) and the noise (figure 3*c*) are enhanced compared to the homogeneous case (shown in figure 1). In addition, the DNR of this subpopulation essentially replicates the behaviour of the homogeneous case (figure 1*f*): minimum near criticality, and larger values for the subcritical compared with the supercritical regime (figure 3*d*). Notably, in the presence of diversity the dynamic range at criticality for the subpopulation with $\theta = 1$ is enhanced. Yet, as the noise is enhanced even more for this subpopulation, the DNR is minimal.

3.4. Combining critical sensitivity with subcritical specificity

The response of the critical subpopulation has enhanced sensitivity but compromised specificity, and the responses of the subcritical subpopulations have lower sensitivity but improved specificity. These specialized responses allow for the possibility of combining the optimal features of the output of each group that coexist in heterogeneous systems (figure 4*a*). To explore this avenue, it is first convenient to split the network into three groups: (i) the subpopulation of most excitable elements ($\theta = 1$), (ii) the whole network and (iii) the union of all integrators ($\theta > 1$). These groups exhibit distinct properties with (i) and (iii) showing opposite features and (ii) representing a middle ground between them. The most excitable group (i) and the whole network (ii) show peaks for both dynamic range and noise at p_c^1. This is in contrast to integrators (iii) that exhibit smooth curves (without peaks) for both dynamic range and noise because they are in the subcritical regime (blue lines, figures 4*b*,*c*).

By exploring the differences among subpopulations, the DNR is estimated combining the sensitivity of groups (i) and (ii), Δ^1 and Δ^T, with the specificity of the three groups (Σ^x, figure 4*d*,*e*). Marrying the dynamic range of group (i) with the noise of group (iii) leads to maximal DNR at criticality (figure 4*d*). Thus, optimal sensitivity can coexist with the maximal DNR when the estimations of the dynamic range and the noise come from segregated groups.

Comparing the DNR at criticality across groups demonstrates the advantage of diversity with respect to homogeneous networks (figure 4*f*). This proof-of-principle comparison reveals the importance of combining integration and segregation [46,47] of heterogeneous groups as illustrated in the generic scheme of figure 4*a*: Integration occurs within the network as nodes interact with nodes from other subpopulations (purple arrows); segregation corresponds to the separation of the outputs from critical and subcritical subpopulations of the primary level towards a secondary level (red and blue arrows). Enhanced sensitivity occurs only in one subpopulation ($\theta = 1$). And the optimal DNR requires the dynamic range of the critical

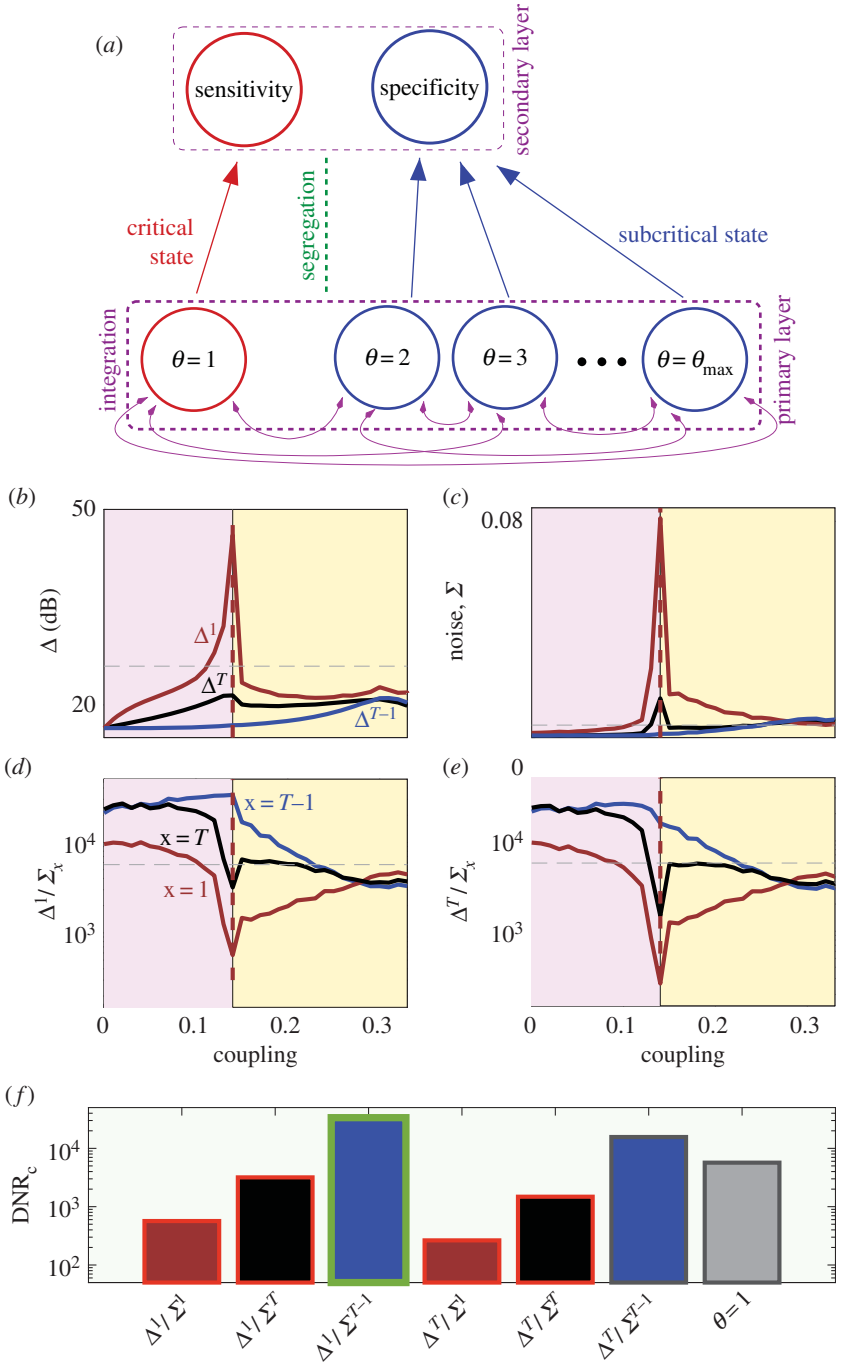

Figure 4. Combining critical sensitivity with subcritical specificity. (*a*) Minimal two-level hierarchical structure with horizontal integration (within layer) and vertical segregation (between layers). (*b*) Dynamic range versus coupling strength p for the most excitable subpopulation Δ^1, the average of all subpopulations Δ^T and the average of all integrators Δ^{T-1}. (*c*) Noise versus p for the same groups: Σ^1 (most excitable, red), Σ^T (all, black), Σ^{T-1} (integrators, blue). (*d*) Dynamic-range-to-noise ratio combining the dynamic range from Δ^1 with the noise from the other groups. (*e*) Dynamic-range-to-noise ratio combining the dynamic range from Δ^T with the noise from the other groups. Horizontal dashed lines indicate critical values for the homogeneous system of figure 1. Red dashed lines indicate p_c^1. (*f*) Comparison of the above results for the dynamic-range-to-noise ratio at criticality with the homogeneous case $\theta = 1$ (grey). Red borders denote a minimum and the green border denotes a maximum of the DNR at criticality. (Online version in colour.)

subpopulation and the noise of subcritical subpopulations. Without this separation, heterogeneous networks perform worse than homogeneous networks for dynamic range (Δ^T in figure 4*b*), noise (Σ^T in figure 4*c*) and the DNR (Δ^T/Σ^T in figures 4*e*,*f*). To behave optimally, the system needs to take advantage of the best feature of each subgroup.

4. Discussion

The importance of critical systems is now widely established [19,48–51]. More recently, enhanced consistency and stability of subcritical systems have also been recognized as important features [39–41]. In addition to affecting the dynamics of systems [35,52,53] and improving performance in several aspects [34,36], nodal heterogeneity can also lead to functional diversity in which the dynamics of subgroups are tuned to different dynamical regimes. Compared with homogeneous systems, functional diversity can furnish several simultaneous advantages. (i) Specificity is enhanced in subcritical subpopulations because their response is more reliable and less variable. (ii) Sensitivity is enhanced in the critical subpopulation because these nodes are more excitable (stronger critical coupling) and, thus, more effective in amplifying weak stimuli (without

significant early saturation for strong stimuli). (iii) The ratio between the critical sensitivity (dynamic range) and the subcritical variability (noise) is maximized. Adding to the ever-growing list of advantages of diversity [54,55], we find that functional diversity can promote the coexistence of enhanced specificity with optimal sensitivity and maximal DNR.

To take advantage of features of critical and subcritical regimes, we propose a simple hierarchical organization [56–60] that segregates and integrates the activity of the subpopulations, which are two major processes of complex dynamics [46,61]. The proposed structure, illustrated in figure 4*a*, involves integration among heterogeneous elements, and segregation of the output from critical and subcritical groups towards higher hierarchical levels. At the bottom of the hierarchy, integration only requires recurrent connections, and segregation requires the separation of the different responses. A future task consists in elucidating the precise mechanism in which neurons at the top of the hierarchy optimally associate inputs from critical and subcritical sources. Growing evidence indicates that this separability leads to an exquisite level of specialization observed in neuronal activity [62,63], including regions responding to stimulus noise or prediction error [64]. Given the specialization of brain activity, which is most widely found in neuroimaging experiments [65], it is reasonable to expect that the sensitivity and specificity of subnetwork responses are separable features that can be combined to generate an accurate DNR estimation. Likewise, more sophisticated combinations of features should also occur from heterogeneous responses.

The appealing critical-brain hypothesis has been proposed as a method that would allow the brain to take advantage of several features that are optimized at criticality [66–68]. However, despite clear benefits for information processing, this hypothesis remains controversial, particularly as numerous evidences of non-critical dynamics also exist [39–41]. By revealing that the advantages of critical systems only require a small proportion of critical units, our findings reconcile these two points of view. Hence, experiments may highlight critical and/or subcritical aspects of the dynamics because these regimes are not exclusive. Moreover, the coexistence of subcritical and critical subparts of a system can optimize the collective response.

In summary, we propose a mechanism that allows a critical system to overcome the limitations of enhanced critical fluctuations, improving specificity, optimizing sensitivity and maximizing the DNR, which reflects a trade-off between sensitivity and specificity. The proposal requires functional diversity and separated pathways that are responsible for conveying complementary representations of the network response: sensitivity from critical elements and specificity from subcritical ones. The benefits of functional diversity are likely (i) to find further applications because they allow for the combination of multiple specialized features, and (ii) to transfer to a variety of systems because heterogeneity is ubiquitous in nature.

Data accessibility. This article has no additional data.

Competing interests. We declare we have no competing interests.

Funding. This work was supported by the Australian Research Council and the Australian National Health and Medical Research Council (APP1110975).

Acknowledgments. I thank M. Copelli, J. Roberts, M. Breakspear and the Systems Neuroscience Group for helpful discussions, and anonymous reviewers for their thoughtful help in presenting these ideas.

References

1. VonNeumann J. 1956 Probabilistic logics and the synthesis of reliable organisms from unreliable components. *Autom. Stud.* **34**, 43–98.
2. Rieke F. 1999 *Spikes: exploring the neural code*. Cambridge, MA: MIT Press.
3. Faisal AA, Selen LPJ, Wolpert DM. 2008 Noise in the nervous system. *Nat. Rev. Neurosci.* **9**, 292–303. (doi:10.1038/nrn2258)
4. Bray D, Levin MD, Morton-Firth CJ. 1998 Receptor clustering as a cellular mechanism to control sensitivity. *Nature* **393**, 85–88. (doi:10.1038/30018)
5. Gollo LL, Kinouchi O, Copelli M. 2009 Active dendrites enhance neuronal dynamic range. *PLoS. Comput. Biol.* **5**, e1000402. (doi:10.1371/journal.pcbi.1000402)
6. Stevens SS. 1975 *Psychophysics: introduction to its perceptual, neural and social prospects*. New York, NY: Wiley.
7. Laplace PS. 2012 *Pierre-Simon laplace philosophical essay on probabilities*. (Transl. from the fifth French edition of 1825 with notes by the translator), vol. 13. Berlin, Germany: Springer Science & Business Media.
8. Ayton P, Fischer I. 2004 The hot hand fallacy and the gambler's fallacy: two faces of subjective randomness?. *Mem. Cognit.* **32**, 1369–1378. (doi:10.3758/BF03206327)
9. Lawson RP, Mathys C, Rees G. 2017 Adults with autism overestimate the volatility of the sensory environment. *Nat. Neurosci.* **20**, 1293–1299. (doi:10.1038/nn.4615)
10. Cavagna A, Cimarelli A, Giardina I, Parisi G, Santagati R, Stefanini F, Viale M. 2010 Scale-free correlations in starling flocks. *Proc. Natl Acad. Sci. USA* **107**, 11 865–11 870. (doi:10.1073/pnas.1005766107)
11. Stanley HE. 1987 *Introduction to phase transitions and critical phenomena*. Oxford, UK: Oxford University Press.
12. Haldeman C, Beggs JM. 2005 Critical branching captures activity in living neural networks and maximizes the number of metastable states. *Phys. Rev. Lett.* **94**, 058101. (doi:10.1103/PhysRevLett.94.058101)
13. Mosqueiro TS, Maia LP. 2013 Optimal channel efficiency in a sensory network. *Phys. Rev. E* **88**, 012712. (doi:10.1103/PhysRevE.88.012712)
14. Lizier JT, Prokopenko M, Zomaya AY. 2010 Information modification and particle collisions in distributed computation. *Chaos* **20**, 037109. (doi:10.1063/1.3486801)
15. Shew WL, Yang H, Yu S, Roy R, Plenz D. 2011 Information capacity and transmission are maximized in balanced cortical networks with neuronal avalanches. *J. Neurosci.* **31**, 55–63. (doi:10.1523/JNEUROSCI.4637-10.2011)
16. Williams-García RV, Moore M, Beggs JM, Ortiz G. 2014 Quasicritical brain dynamics on a nonequilibrium widom line. *Phys. Rev. E* **90**, 062714. (doi:10.1103/PhysRevE.90.062714)
17. Vázquez-Rodríguez B, Avena-Koenigsberger A, Sporns O, Griffa A, Hagmann P, Larralde H. 2017 Stochastic resonance and optimal information transfer at criticality on a network model of the human connectome. (http://arxiv.org/abs/1705.05248).
18. Langton CG. 1990 Computation at the edge of chaos: phase transitions and emergent computation. *Phys. D* **42**, 12–37. (doi:10.1016/0167-2789(90)90064-V)
19. Cocchi L, Gollo LL, Zalesky A, Breakspear M. In press. Criticality in the brain: a synthesis of neurobiology, models and cognition. *Prog. Neurobiol*. (doi:10.1016/j.pneurobio.2017.07.002)
20. Kinouchi O, Copelli M. 2006 Optimal dynamical range of excitable networks at criticality. *Nature Phys.* **2**, 348–351. (doi:10.1038/nphys289)
21. Gollo LL, Kinouchi O, Copelli M. 2013 Single-neuron criticality optimizes analog dendritic computation. *Sci. Rep.* **3**, 3222. (doi:10.1038/srep03222)

22. Plenz D, Niebur E. 2014 *Criticality in neural systems*. New York, NY: John Wiley & Sons.
23. Scheffer M *et al.* 2009 Early-warning signals for critical transitions. *Nature* **461**, 53–59. (doi:10.1038/nature08227)
24. Gal A, Marom S. 2013 Self-organized criticality in single-neuron excitability. *Phys. Rev. E* **88**, 062717. (doi:10.1103/PhysRevE.88.062717)
25. Shew WL, Clawson WP, Pobst J, Karimipanah Y, Wright NC, Wessel R. 2015 Adaptation to sensory input tunes visual cortex to criticality. *Nat. Phys.* **11**, 659–663. (doi:10.1038/nphys3370)
26. Publio R, Oliveira RF, Roque AC. 2009 A computational study on the role of gap junctions and rod I_h conductance in the enhancement of the dynamic range of the retina. *PLoS ONE* **4**, e6970. (doi:10.1371/journal.pone.0006970)
27. Eguíluz VM, Ospeck M, Choe Y, Hudspeth AJ, Magnasco MO. 2000 Essential nonlinearities in hearing. *Phys. Rev. Lett.* **84**, 5232. (doi:10.1103/PhysRevLett.84.5232)
28. Camalet S, Duke T, Jülicher F, Prost J. 2000 Auditory sensitivity provided by self-tuned critical oscillations of hair cells. *Proc. Natl Acad. Sci. USA* **97**, 3183–3188. (doi:10.1073/pnas.97.7.3183)
29. Hudspeth AJ. 2008 Making an effort to listen: mechanical amplification in the ear. *Neuron* **59**, 530–545. (doi:10.1016/j.neuron.2008.07.012)
30. Gollo LL, Kinouchi O, Copelli M. 2012 Statistical physics approach to dendritic computation: the excitable-wave mean-field approximation. *Phys. Rev. E* **85**, 011911. (doi:10.1103/PhysRevE.85.011911)
31. Wang CY, Wu ZX, Chen MZQ. 2017 Approximate-master-equation approach for the Kinouchi-Copelli neural model on networks. *Phys. Rev. E* **95**, 012310. (doi:10.1103/PhysRevE.95.012310)
32. Gollo LL, Mirasso C, Eguíluz VM. 2012 Signal integration enhances the dynamic range in neuronal systems. *Phys. Rev. E* **85**, 040902. (doi:10.1103/PhysRevE.85.040902)
33. Nelson SB, Sugino K, Hempel CM. 2006 The problem of neuronal cell types: a physiological genomics approach. *Trends. Neurosci.* **29**, 339–345. (doi:10.1016/j.tins.2006.05.004)
34. Mejias JF, Longtin A. 2012 Optimal heterogeneity for coding in spiking neural networks. *Phys. Rev. Lett.* **108**, 228102. (doi:10.1103/PhysRevLett.108.228102)
35. Padmanabhan K, Urban NN. 2010 Intrinsic biophysical diversity decorrelates neuronal firing while increasing information content. *Nat. Neurosci.* **13**, 1276–1282. (doi:10.1038/nn.2630)
36. Gollo LL, Copelli M, Roberts JA. 2016 Diversity improves performance in excitable networks. *PeerJ* **4**, e1912. (doi:10.7717/peerj.1912)
37. Shadlen MN, Newsome WT. 1994 Noise, neural codes and cortical organization. *Curr. Opin. Neurobiol.* **4**, 569–579. (doi:10.1016/0959-4388(94)90059-0)
38. Cleland TA, Linster C. 1999 Concentration tuning mediated by spare receptor capacity in olfactory sensory neurons: a theoretical study. *Neural Comput.* **11**, 1673–1690. (doi:10.1162/089976699300016188)
39. Priesemann V, Valderrama M, Wibral M, Le Van Quyen M. 2013 Neuronal avalanches differ from wakefulness to deep sleep–evidence from intracranial depth recordings in humans. *PLoS Comput. Biol.* **9**, e1002985. (doi:10.1371/journal.pcbi.1002985)
40. Priesemann V, Wibral M, Valderrama M, Pröpper R, Le Van Quyen M, Geisel T, Triesch J, Nikolić D, Munk MH. 2013 Spike avalanches in vivo suggest a driven, slightly subcritical brain state. *Front. Syst. Neurosci.* **8**, 108. (doi:10.3389/fnsys.2014.00108)
41. Tomen N, Rotermund D, Ernst U. 2015 Marginally subcritical dynamics explain enhanced stimulus discriminability under attention. *Front. Syst. Neurosci* **8**, 151. (doi:10.3389/fnsys.2014.00151)
42. Poil SS, van Ooyen A, Linkenkaer-Hansen K. 2008 Avalanche dynamics of human brain oscillations: relation to critical branching processes and temporal correlations. *Hum. Brain. Mapp.* **29**, 770–777. (doi:10.1002/hbm.20590)
43. Larremore DB, Shew WL, Ott E, Sorrentino F, Restrepo JG. 2014 Inhibition causes ceaseless dynamics in networks of excitable nodes. *Phys. Rev. Lett.* **112**, 138103. (doi:10.1103/PhysRevLett.112.138103)
44. Wang HP, Spencer D, Fellous JM, Sejnowski TJ. 2010 Synchrony of thalamocortical inputs maximizes cortical reliability. *Science* **328**, 106–109. (doi:10.1126/science.1183108)
45. Colomer-deSimón P, Boguñá M. 2014 Double percolation phase transition in clustered complex networks. *Phys. Rev. X* **4**, 041020. (doi:10.1103/PhysRevX.4.041020)
46. Tononi G, Sporns O, Edelman GM. 1994 A measure for brain complexity: relating functional segregation and integration in the nervous system. *Proc. Natl Acad. Sci. USA* **91**, 5033–5037. (doi:10.1073/pnas.91.11.5033)
47. Sporns O. 2010 *Networks of the brain*. Cambridge, MA: MIT press.
48. Roli A, Villani M, Filisetti A, Serra R. 2015 Dynamical criticality: overview and open questions. (http://arxiv.org/abs/1512.05259)
49. Mora T, Bialek W. 2011 Are biological systems poised at criticality? *J. Stat. Phys.* **144**, 268–302. (doi:10.1007/s10955-011-0229-4)
50. Deco G, Jirsa VK. 2012 Ongoing cortical activity at rest: criticality, multistability, and ghost attractors. *J. Neurosci.* **32**, 3366–3375. (doi:10.1523/JNEUROSCI.2523-11.2012)
51. Shew WL, Plenz D. 2013 The functional benefits of criticality in the cortex. *Neuroscientist* **19**, 88–100. (doi:10.1177/1073858412445487)
52. Cartwright JHE. 2000 Emergent global oscillations in heterogeneous excitable media: the example of pancreatic β cells. *Phys. Rev. E* **62**, 1149. (doi:10.1103/PhysRevE.62.1149)
53. Tessone CJ, Mirasso CR, Toral R, Gunton JD. 2006 Diversity-induced resonance. *Phys. Rev. Lett.* **97**, 194101. (doi:10.1103/PhysRevLett.97.194101)
54. Van Knippenberg D, Schippers MC. 2007 Work group diversity. *Annu. Rev. Psychol.* **58**, 515–541. (doi:10.1146/annurev.psych.58.110405.085546)
55. Joshi A, Roh H. 2009 The role of context in work team diversity research: a meta-analytic review. *Acad. Manage. J.* **52**, 599–627. (doi:10.5465/AMJ.2009.41331491)
56. Zeki S, Shipp S. 1988 The functional logic of cortical connections. *Nature* **335**, 311–317. (doi:10.1038/335311a0)
57. Mesulam MM. 1998 From sensation to cognition. *Brain* **121**, 1013–1052. (doi:10.1093/brain/121.6.1013)
58. Felleman DJ, Van Essen DC. 1991 Distributed hierarchical processing in the primate cerebral cortex. *Cereb. Cortex* **1**, 1–47. (doi:10.1093/cercor/1.1.1)
59. Hochstein S, Ahissar M. 2002 View from the top: Hierarchies and reverse hierarchies in the visual system. *Neuron* **36**, 791–804. (doi:10.1016/S0896-6273(02)01091-7)
60. Kiebel SJ, Daunizeau J, Friston KJ. 2008 A hierarchy of time-scales and the brain. *PLoS Comput. Biol.* **4**, e1000209. (doi:10.1371/journal.pcbi.1000209)
61. Fox PT, Friston KJ. 2012 Distributed processing; distributed functions? *Neuroimage* **61**, 407–426. (doi:10.1016/j.neuroimage.2011.12.051)
62. Quiroga RQ, Reddy L, Kreiman G, Koch C, Fried I. 2005 Invariant visual representation by single neurons in the human brain. *Nature* **435**, 1102–1107. (doi:10.1038/nature03687)
63. Gross CG. 2002 Genealogy of the 'grandmother cell'. *Neuroscientist* **8**, 512–518. (doi:10.1177/107385802237175)
64. Iglesias S, Mathys C, Brodersen KH, Kasper L, Piccirelli M, den Ouden HEM, Stephan KE. 2013 Hierarchical prediction errors in midbrain and basal forebrain during sensory learning. *Neuron* **80**, 519–530. (doi:10.1016/j.neuron.2013.09.009)
65. Yarkoni T, Poldrack RA, Nichols TE, Van Essen DC, Wager TD. 2011 Large-scale automated synthesis of human functional neuroimaging data. *Nat. Methods* **8**, 665–670. (doi:10.1038/nmeth.1635)
66. Chialvo DR. 2004 Critical brain networks. *Phys. A* **340**, 756–765. (doi:10.1016/j.physa.2004.05.064)
67. Chialvo DR. 2010 Emergent complex neural dynamics. *Nat. Phys.* **6**, 744–750. (doi:10.1038/nphys1803)
68. Beggs JM. 2008 The criticality hypothesis: how local cortical networks might optimize information processing. *Phil. Trans. R. Soc. A* **366**, 329–343. (doi:10.1098/rsta.2007.2092)